Journal of Thermal Engineering
Web page info: https://jten.yildiz.edu.tr
DOI: 10.18186/thermal.990865

Research Article

Effect of fibrous porous material on natural convection heat transfer from a horizontal circular cylinder located in a square enclosure

Hasan Shakir MAJDI[1], Akeel Abdullah MOHAMMED[2], Amer Abdullah MOHAMMED[3], Laith Jaafer HABEEB[4,*]

[1]*Department of Chemical Engineering and Petroleum Industries, Al-Mustaqbal University College, Babylon, Iraq*
[2]*Department of Mechanical Engineering, Al-Nahrain University, Baghdad, Iraq*
[3]*Department of Mechanical Engineering, Mustansiriyah University, Baghdad, Iraq*
[4]*Training and Workshop Center, University of Technology – Iraq, Baghdad, Iraq*

ARTICLE INFO

Article history
Received: 01 August 2019
Accepted: 17 May 2020

Key words:
Natural convection; Square cavity; Porous media

ABSTRACT

A numerical simulation study was carried out to investigate a steady two-dimensional laminar natural convective heat transfer from a uniformly heated inner circular cylinder placed inside an air-filled square enclosure with a porous material. The enclosure's side and upper walls were isothermal, while the bottom wall was adiabatic. All the numerical calculations were performed in the range of Rayleigh numbers between 10^3 and 10^7. The material porosity (ε), the solid to fluid thermal conductivity ratio (k_r), and Darcy number in the present study were 1.0, 0.5, and 0.01, respectively. The results showed that for Rayleigh numbers that are less than 10^6, the isotherms are almost parallel inside the three cold walls except for the corners of the adiabatic bottom wall. The rates of vertical velocity are higher than the horizontal velocity, especially at higher Grashof numbers. Also, the use of fibrous porous material with low thermal conductivity relative to the fluid thermal conductivity reduces the values of average Nusselt number, in addition to reducing the horizontal and vertical velocities along the horizontal axis.

Cite this article as: Majdi HS, Mohammed AA, Mohammed AA, Habeeb LJ. Effect of Fibrous Porous Material on Natural Convection Heat Transfer from a Horizontal Circular Cylinder Located in a Square Enclosure. J Ther Eng 2021;7(6):1468–1478.

INTRODUCTION

Natural convection heat transfer flow in enclosures has received important attention by many researchers [1–15]. Many technological applications are associated with different domain fields and operating conditions, such as medical sciences, geothermal storage, pollution, food technology, fire protection techniques, hazardous thermochemical spreading, building insulation, and solar heating of electronic devices. The existing enclosure aims to decrease the rate of heat transfer from the hot inner surface or to

***Corresponding author.**
*E-mail address: Laith.J.Habeeb@uotechnology.edu.iq

This paper was recommended for publication in revised form by Regional Editor Sandip Kale

protect the inner body when it is exposed to a harsh outdoor environment. The annular region can be geometrically formed by an inner cylinder with any geometry (circular, square, elliptic, etc.) or inner flat plate enclosed by rectangular, elliptical, or circular cylinder, i.e., two concentric or eccentric annulus with identical or different geometries. Amaresh and Manab [1] studied the laminar natural convection in an inclined complicated cavity with three cold flat walls and one wavy wall having a sinusoidal temperature profile. It was concluded that the average heat transfer rate on the wavy wall with an increase in the amplitude is significantly high at low Rayleigh numbers. Ding et al. [2] studied the influence of the geometric parameters, such as angular positions and eccentricities on the mean and rates of the local heat transfer in a horizontal eccentric annulus between a heated circular inner cylinder and a square outer cylinder. Ahmed et al. [3] investigated the influence of a single and multiple partitions on the phenomena of natural convection in a differentially heated square cavity with different angles of inclination. Results depicted that the heat transfer process decreases when the number of partitions attached to the cold wall of the enclosure increases. Also, Yasin et al. [4] studied the same phenomenon in a right-triangular enclosure with a solid square body placed remote from the origin with a 0.3 distance in the vertical and horizontal directions. It was inferred that the fluid flow and the heat transfer vigorously rely on the body's thermal boundary conditions. Abdullatif and Ali [5] focused on the conjugate free convection heat transfer in a square enclosure has one thin heated vertical wall of arbitrary thermal conductivities and three thick cooled walls. A heated inclined thin fin of three arbitrary lengths was attached in the middle of the enclosure. It was concluded that the inclination angle and length of the thin fin and the thermal conductivity ratio between solid and fluid have significant effects on the overall heat transfer coefficient of the heated surfaces of the system. Hakan and Eiyad [6] investigated the natural convection heat transfer in a partially heated rectangular enclosure using nanofluids with various volume fractions. The right vertical wall temperature was less than that one for the heater, whereas the rest of the walls were insulated. It was deduced that the average heat transfer rate increases with increasing the volume fraction of nanoparticles for the whole range of Rayleigh numbers. Xu Xu et al. [7] investigated another geometry consisted of a horizontal annulus between a heated inclined triangular cylinder and its circular cylindrical enclosure for wide ranges of Rayleigh numbers and different radius ratios. It was concluded that at a constant radius ratio, there is no effect for the inclination angles of the inner triangular cylinder on the average heat transfer. Salam and Ahmed [8] used a consistent heat source subjected to the inner circular cylinder inside a square enclosure filled with air. All the taken boundaries were assumed isothermal. It was found that the total average Nusselt number behaves nonlinearly as a function of locations. Zi-Tao et al. [9] studied the unsteady natural convection heat transfer in a horizontal heated inner circular cylinder enclosed by a coaxial triangular enclosure for different values of aspect ratios and angles of the enclosure inclination. The presence of different phases during the flow development through the growth of the average Nusselt number over the inner wall surface was observed. Shekholeslami et al. [10] investigated the effect of magnetic field on the natural convection in a curved-shape enclosure. It was found that the Nusselt number decreases as the Hartmann number increases. Balamurugan and Krishnakanth [11] used square and triangle bars of hot sources located inside a square enclosure having cold vertical walls and insulated horizontal walls based on using the air as a medium. It was concluded that the square source gives a higher heat transfer rate than that given by the triangle source. Ravnik and Škerget [12] used Cu, Al_2O_3 and TiO_2 nanofluid as a medium to study the free convection heat transfer in an inclined cooled cubic enclosure with a heated circular and an ellipsoidal cylinder. The results showed that when convection is the dominant heat transfer mechanism, the use of nanofluids yields a smaller increase in the heat transfer efficiency. Raju et al. [13] utilized a saturated porous medium with an insulated circular body in the presence of a heat generation inside a triangular enclosure. The triangular cylinder bottom wall was heated at a fixed temperature, whereas the cavities to the left and right of the inclined walls were kept at a cold temperature. It was concluded that the heat generation effect is negligible for the large size of the circular body. Xing et al. [14] used different geometries for the inner cylinder (circular, elliptical, square, and triangular cylinder) inside a circular enclosure with or without surface radiation. It was noted that the surface radiation resulted from the relatively higher Rayleigh numbers, and the presence of corners with a larger top space enhances the heat transfer rate. Yen et al. [15] analyzed the steady and unsteady natural convection in a cubical enclosure with different inner circular cylinder positions. The air was the medium fluid. The location of the inner cylinder was changed vertically along the centerline of the enclosure. The results revealed that the effect of the boundary wall on the characteristics of fluid flow and heat transfer in the enclosure depends on both the position of the cylinder and the Rayleigh number value. Krunal and Manikandan [16] studied these phenomena in a square enclosure with a heated hexagonal block for non-Newtonian power law fluids. The thermal boundary conditions of a hexagonal block are a constant wall temperature or a uniform heat flux. The results manifested that a higher heat transfer rate can be achieved by using a uniform heat flux condition. Masoud et al. [17] used copper oxide and multi-walled carbon nanotubes to experimentally enhance the thermal conductivity of water. All the thermal conductivity measurements were done in the range of 25–50 °C. It was shown that the thermal conductivity of the nanofluid increases with

temperature at more solid concentration. Ammar et al. [18] focused on the effect of aspect ratio and wall thickness in a porous enclosure with partially heated vertical walls and adiabatic horizontal walls. They concluded that decreasing the wall thickness and aspect ratio leads to improving the heat transfer. Pekmen [19] used Fe_3O_4-water with porous media inside square cavity subjected to magnetic field at the left wall to show that the natural convection heat transfer enhances with increase in volume fraction and Rayleigh number and it is inhibited as Hartmann umber increases and Darcy number decreases. Iman Ataei et al. [20] have experimentally studied the natural convection heat transfer inside the enclosure with a heated bottom and cooled top walls, filled with large solid spheres. The heat transfer measurements showed that at higher Rayleigh number values, the Nusselt number is higher than that for pure Rayleigh-Bénard convection. This depends on the on-packing size and thermal conductivity of the used spheres. Iman Zahmatkesh and Razieh Akhlaghi [21] used the visualization technique to investigate numerically the effect of magnetic field on natural convection inside square cavity contains several water-based nanfluids. They concluded that increase inclination angle of magnetic field reduces the reverse effect of magnetic field increasing on the heat transfer rate.

In this research, the problem of the natural convection heat transfer of a uniformly heated circular cylinder with an enclosed square enclosure has been studied theoretically. The enclosure contains the air with and without fibrous porous material. The main aim of this study is to find out the effect of addition of porous media to the fluid at relatively low thermal conductivity, porosity, and Darcy number on the heat transfer process. The numerical simulations of the problem have been conducted at $Ra = 10^3$–10^7. Streamlines, isotherms contour, velocity distribution, temperature distribution, and average Nusselt number have been determined and discussed.

PHYSICAL MODEL AND NUMERICAL METHOD

Physical Model and Governing Equations

Figure 1 depicts the schematic diagram of the investigated physical domain and coordinate systems. The side and upper three cold walls of the outer rectangular cylinder are maintained at T_c. Also, the bottom wall is insulated, while the inner hot circular cylinder is maintained at T_h.

In the present work, the porous medium is taken as homogeneous and isotropic. The solid matrix is saturated with air within the porous medium to obtain local thermodynamic equilibrium. The flow is assumed to be steady, laminar, incompressible, and two-dimensional. The thermophysical properties of the air and the porous medium are assumed to be constant, except the density in the buoyancy term in the momentum equations at which the density varies linearly according to Boussinesq approximation. The dimensionless governing equations for the fluid without porous medium are:

$$\nabla \cdot U = 0 \tag{1}$$

$$(U \cdot \nabla U) = -\nabla P + Pr \cdot (\nabla^2 U) + Gr \cdot Pr^2 \cdot \theta \tag{2}$$

$$(U \cdot \nabla \theta) = (\nabla^2 \theta), \tag{3}$$

The dimensionless momentum and energy equations for the natural convection heat transfer with porous material are given as follows:

$$\frac{1}{\varepsilon^2}(U.\nabla U) = -\nabla P - \frac{Pr}{Da}U - \frac{C_f}{\sqrt{Da}}\left|\vec{U}\right|U + \frac{Pr}{\varepsilon}\cdot(\nabla^2 U) + Gr.Pr^2 \cdot \theta, \tag{4}$$

$$\varepsilon(U.\nabla\theta) = \frac{k_{f.eff}}{k_f}(\nabla^2\theta), \tag{5}$$

where,

$$\frac{k_{f.eff}}{k_f} = \left(1 - \sqrt{1-\varepsilon}\right) + \frac{2\sqrt{1-\varepsilon}}{1-\lambda B} \times \left[\frac{(1-\lambda)B}{(1-\lambda B)^2}\ln(\lambda B) - \frac{B+1}{2} - \frac{B-1}{1-\lambda B}\right], \tag{6}$$

$$\lambda = \frac{1}{k_r}, \text{ and } B = 1.25\left[\frac{1-\varepsilon}{\varepsilon}\right]^{(10/9)}$$

$$k_r = \frac{k_s}{k_f}$$

$$C_f = \text{inertia coefficient} = \frac{1.75}{150\varepsilon^3} \tag{7}$$

The local rate of heat transfer is calculated by the Fourier's law:

$$q_f = -\frac{k_{f.eff}}{k_f}\frac{\partial T}{\partial n} \tag{8}$$

The local Nusselt number is

$$Nu_f = \frac{q_f d}{(T_h - T_c)} \tag{9}$$

The average Nusselt number is calculated by integrating the local Nusselt number along the cylinder as follows:

$$Nu = \frac{1}{s}\int_0^s \frac{k_{f.eff}}{k_f}\frac{\partial \theta_f}{\partial n}ds \tag{10}$$

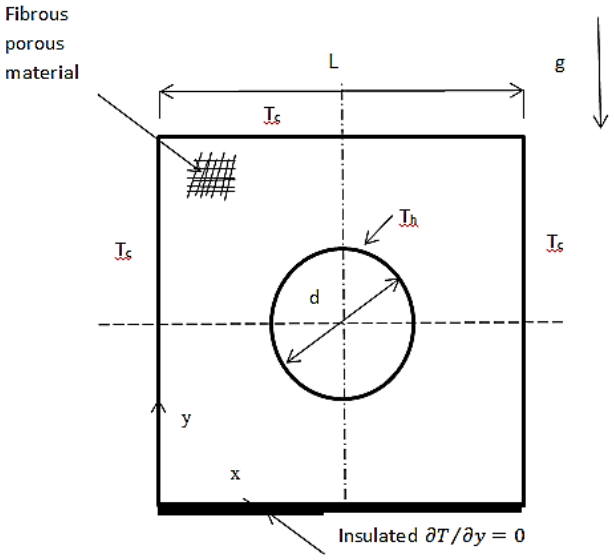

Figure 1. The schematic diagram of the physical domain and coordinate systems.

Rayleigh number is calculated based on the cylinder diameter:

$$Ra = \frac{g\beta d^3 (T_h - T_c)}{\alpha_f \vartheta_f} \tag{11}$$

As can be seen in the above equations, three critical parameters govern the present work, which are the Prandtl, Grashof, and Darcy numbers. The air is the medium fluid (Pr = 0.71), and Darcy number (Da) equals to 0.01. The Rayleigh number varies from 103 to 107, for ensuring the flow is laminar and to meet the steady-state condition. In addition, the material porosity (ε) and the solid to fluid thermal conductivity ratio (k_r) in the present study are 0.5 and 0.1, respectively. No-slip boundary conditions are holding along both the inner and outer walls.

The spectral-element approach was employed for numerically solving the two-dimensional unsteady Navier-Stokes and energy equations, with buoyancy treated via the Boussinesq's approximation.

Computational Details

The governing equations regime has been solved numerically utilizing Galerkin finite element approach based on the spectral element method, which was documented by Fletcher [22]. The computational domain in this method is usually subdivided roughly into a series of 448 separate macro-elements, as manifested in Fig. (2-a). Then, the interior nodes to each macro-element can be generated within the run and spread in accordance with the Gauss-Legendre-Lobatto quadrature. So, the simulation accuracy can be enhanced via increasing the polynomial order (N × N), where (N) is the interior nodes number of the quadrature.

Numerical runs were performed to secure that the numerical outcomes determined are the grid resolution-independent. The study of grid resolution of the computational domain shown in table 1 reveals that the Nusselt number is converged by (7 × 7) nodes internal to every macro-element to become a totally 9600 micro-elements with a relative error of less than 0.4%, as evinced in Fig. (2-b).

Code Validation

Due to the lack of available experimental and theoretical data for the horizontal concentric annulus with identical thermal boundary conditions involved in the current study, benchmarking outcomes by Ding et al. [2] and Salam and Ahmed [8] were utilized to validate the current code

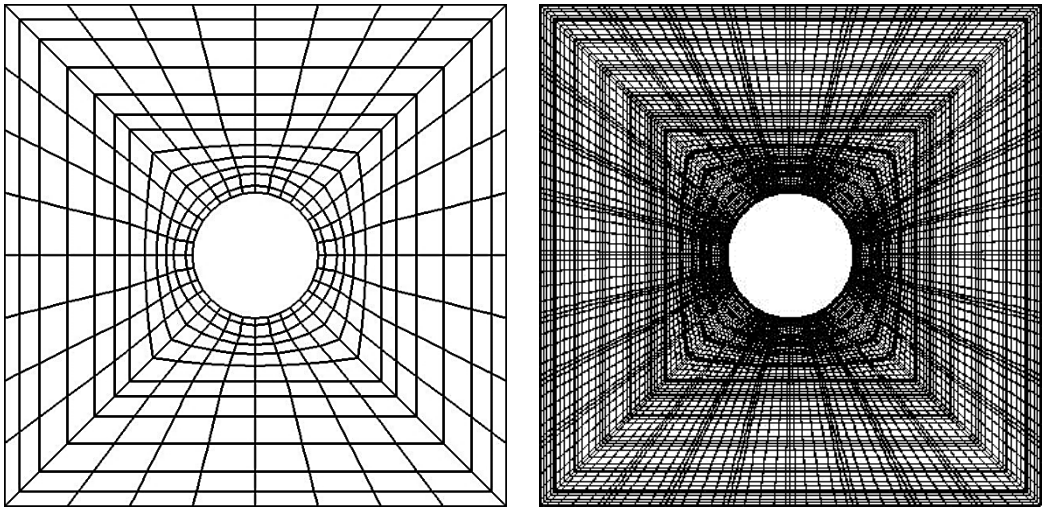

(a) 448 macro-elements (b) 9600 micro-elements

Figure 2. Physical domain and an illustrative grid network generated.

Table 1. Grid resolution results of the computational domain for the average Nusselt number at two Rayleigh numbers (Ra = 10^4 and 10^7)

Mesh size (N × N)	Ra = 10^4	Ra = 10^7
	Nu	
(3 × 3)	1.8898285	4.3125391
(4 × 4)	1.8833322	4.3091521
(5 × 5)	1.8775468	4.3034400
(6 × 6)	1.8737696	4.2986013
(7 × 7)	1.8711568	4.2943479
(8 × 8)	1.8696486	4.2928149

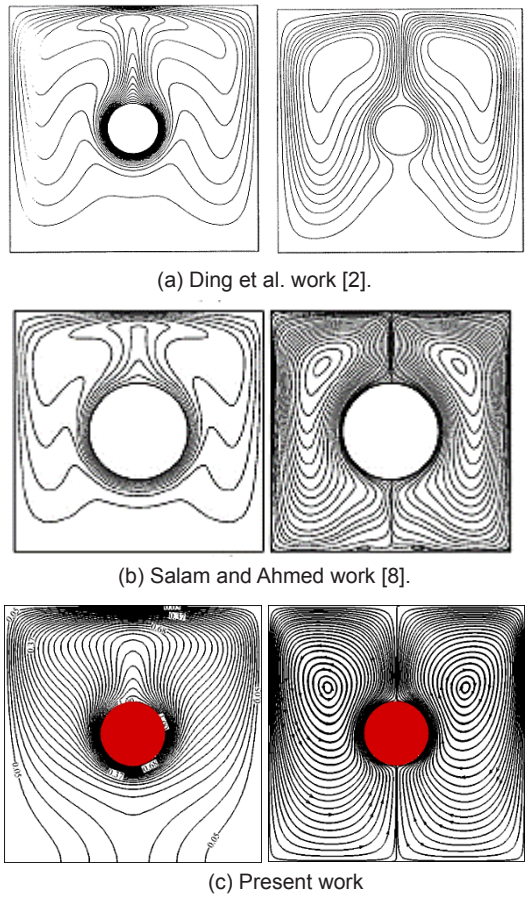

(a) Ding et al. work [2].

(b) Salam and Ahmed work [8].

(c) Present work

Figure 3. Code Validation, Ra = 10^6.

for streamlines and isotherms contours, respectively, as shown in Fig. 3. The thermal boundary conditions of the two previous works are the same as that in the present study except that the outer square cylinder bottom wall is kept at a fixed temperature (T_c). The case of Ra = 10^6 with different radius ratios was selected for the comparison purpose. The medium fluid, the computational domain, and the hydrodynamic boundary conditions in the current code were put to be similar to those in the benchmarking works. As can be noticed in Fig. 3, the behavior and trend of the temperature field and flow pattern for all works are the same only at the upper part of enclosure because of the different thermal boundary conditions at the bottom wall of the enclosure. The circulation of the flow shows the two overall rotating symmetric eddies inside each one of the left and right eddies. The vortices intensity seems to be stronger in the present work than that in the previous works [2, 8], because of the adiabatic bottom wall prevents the heat transfer from this position, so the temperature of this wall will be higher than the other walls. This leads to warm the air particles at the lower part of the enclosure. Table 2. gives identical results of the present code with the results of Pop et al. [23], Yih [24] and Kumari and Jayanthi [25] for local angular heat transfer $\frac{Nu}{\sqrt{Ra}}$ at a circular cylinder surface, for the case of free convection from a circular cylinder located in a porous medium at Ra = 10^3.

RESULTS AND DISCUSSION

This study was initially carried out for the case of natural convection heat transfer outside a heated circular cylinder

Table 2. Comparison for local angular heat transfer at a circular cylinder surface between the results of the current code with the results of Pop et al. [23], Yih [24] and Kumari and Jayanthi [25], for the case of free convection from a circular cylinder located in a porous medium

φ (rad)	Local angular heat transfer $Nu/\sqrt{Ra}$			
	Present work	[23]	[24]	[25]
0	0.62766	0.6272	0.6276	0.6274
0.2	0.62454	0.6295	0.6245	0.6245
0.4	0.61518	0.6202	0.6151	0.6151
0.6	0.59964	0.6048	0.5996	0.5996
0.8	0.57817	0.5834	0.5781	0.5781
1.0	0.55083	0.5562	0.5508	0.5509
1.2	0.51807	0.5236	0.5180	0.5181
1.4	0.48009	0.4859	0.4800	0.4801
1.6	0.43728	0.4433	0.4371	0.4374
1.8	0.38999	0.3964	0.3899	0.3903
2.0	0.33882	0.33882	0.3387	0.3393
2.2	0.28445	0.2913	0.2843	0.2849
2.4	0.22722	0.2339	0.2271	0.2276
2.6	0.16778	0.1741	0.1677	0.1681
2.8	0.10660	0.1119	0.1066	0.1068
3	0.04461	0.0477	0.0446	0.0445
π	0.00011	0.0005	0.0001	0.0001

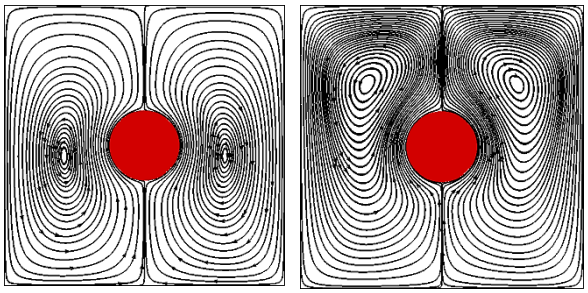

(a) Ra = 10^3

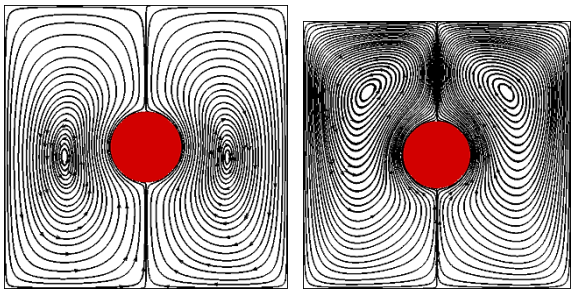

(b) Ra = 10^4

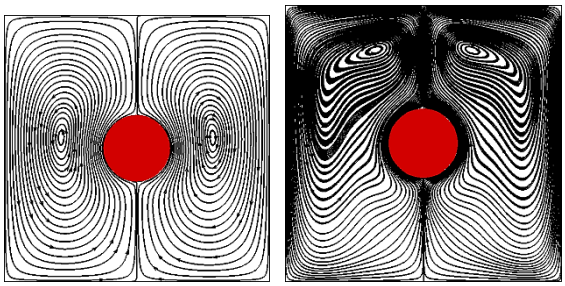

(c) Ra = 10^5

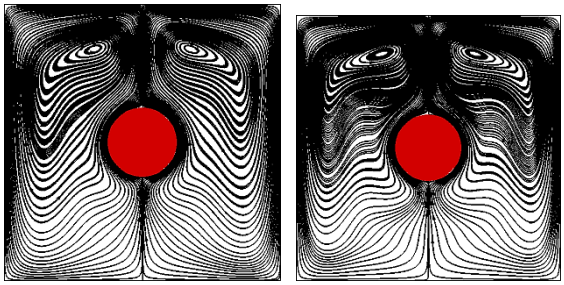

(d) Ra = 10^6

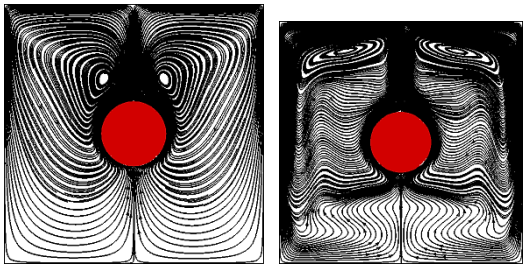

(e) Ra = 10^7

Figure 4. The streamlines contours without porous materials (left) and with porous material (right) at different values of Rayleigh number.

enclosed by a square cavity with a constant Prandtl number Pr = 0.7 (air). Constant radius ratio was taken (RR = 3.5), and five different Rayleigh numbers (Ra = 10^3, 10^4, 10^5, 10^6 and 10^7) were considered. Then, the same study is repeated but for the case of an enclosure filled with a fibrous porous material.

Streamline Maps

The variation of streamlines contours at different values of Rayleigh number around a heated circular cylinder enclosed by an air-filled square enclosure with a porous material (right) and without fibrous porous material (left) are illustrated in Fig. 4. As shown in the left side figure, when the enclosure is filled with air only without fibrous porous material, there are two rotating vortices cover the filled enclosure and move in an opposite direction close to the enclosure sidewalls. Gradually, the center of vortices moves from the centerline of enclosure towards the upper part as Rayleigh number increases. This is due to the increase of flow circulation intensity with increase Rayleigh number lead to an increase of the buoyancy currents. By adding the fibrous porous materials into the enclosure as shown in the right side of Fig. 4, the results elucidate that at the same low value of Rayleigh number (10^3 and 10^4), the center of vortices lies at the upper part of the enclosure. The vortices will be intensive as the Rayleigh number increases more than 104. Besides, the two centers of vortices close to each other and nearly merge at Ra=10^7 due to the high permeability of porous medium is leading to an increase of the resistance against the fluid. This gives sharp vortex than that without porous material. The flow at the bottom of the enclosure is too weak in comparison with that at the middle and top zones, which results in stratification influences in the lower part of the enclosure.

Isotherms Map

Figure 5 explains the distribution of thermal fields (isotherms) in the square enclosure with and without fibrous porous material (right and left), respectively. This figure shows that on the right side, the hot air near to the surface of the heated inner circular cylinder moves upward and hits the three isothermal cold upper and side surfaces of the square cavity. Then, it changes its direction down towards the adiabatic wall producing rotating symmetrical vortices. As can be seen in this figure, when the Rayleigh numbers are less than 10^6, the isotherms are almost parallel inside the three cold walls except for the corners of the adiabatic bottom wall. Here, the dominated mode of heat transfer in the enclosure is almost the conduction. The temperature contours become more confused with increasing Rayleigh number. As a result, the flow vigorously hits the top wall surface of the square enclosure, and a thin thermal boundary layer will be formed in this region. The isotherms will travel upward, and the heat transfer is owing to the natural convection, see reference [8]. When the Rayleigh number becomes more than (10^5), the effect of convection

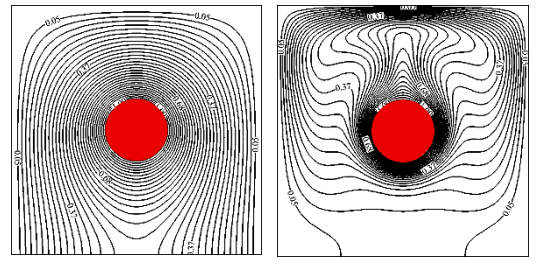

(a) Ra = 10^3

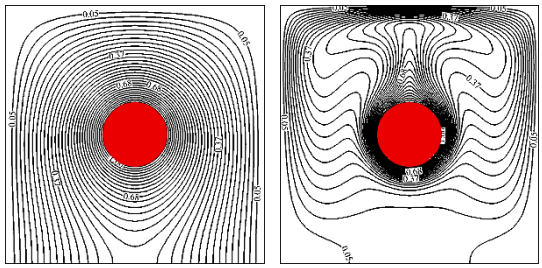

(b) Ra = 10^4

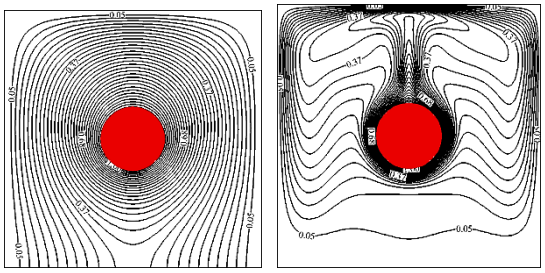

(c) Ra = 10^5

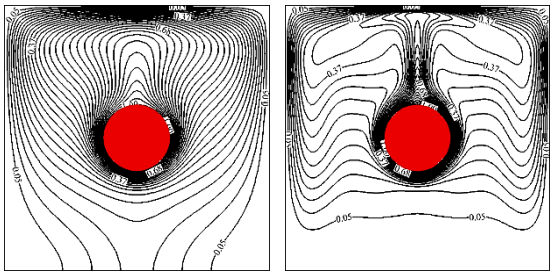

(d) Ra = 10^6

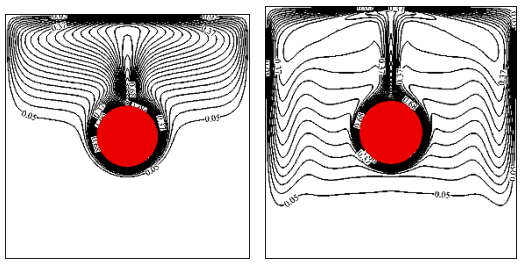

(e) Ra = 10^7

Figure 5. The isotherms contour without porous materials (left) and with porous material (right) at various Rayleigh numbers.

heat transfer becomes more important, and the thermal boundary layer above the inner cylinder surface gets thinner. In addition, a plume begins to appear upon the top of the inner cylinder. Hence, when the enclosure is filled with fibrous porous material, the convection heat transfer becomes stronger even at the lower values of Rayleigh number, and the plume begins to appear upon the top of the inner cylinder with increasing the heat transfer rates when the Rayleigh number rises.

The Average Nusselt Number and Correlation

The average Nusselt number is used for representing the total rate of heat transfer within the domain of interest. The variation of the average Nusselt number versus Grashof number for a hot circular cylinder within a square cavity filled with air only or with fibrous porous material is shown in Fig. 6. For the first case, from Gr = 10^3 to Gr = 10^6, the curves are nearly flat due to the slight contribution of the natural convection to the total heat transfer, and the heat conduction is prevailing in this regime. Nevertheless, for Grashof number more than 106, the average Nusselt numbers are significantly increased and become almost three times that at Gr = 103, which demonstrates an essential improvement of the total heat transfer via the natural convection. It can also be observed that for Grashof number higher than 10^3, the rate of heat transfer in the case of the cavity without porous material is higher than that with a porous material because of the low thermal conductivity of porous material relative to the fluid ($k_s = k_f$). Also, at constant Grashof number, the low value of Darcy number (Da = 10^{-2}) leads to an impermeable medium, which means slow motion of natural convection. As a result, decreasing

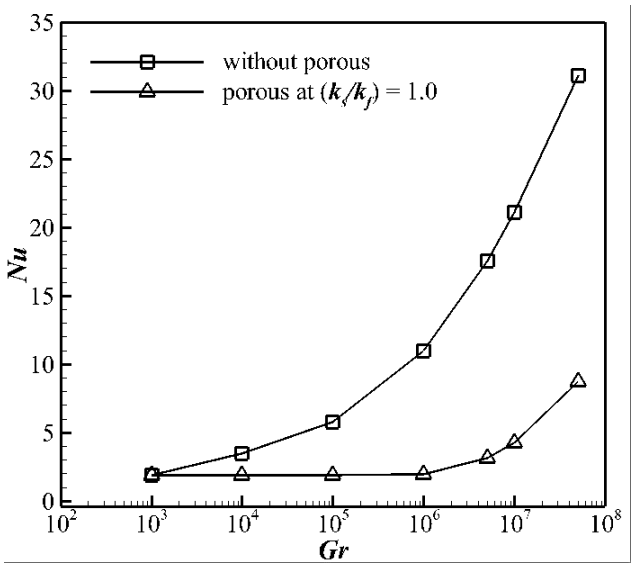

Figure 6. Variation of the average Nusselt number versus Grashof number for a hot circular cylinder in a square cavity with and without fibrous porous material at (k_s/k_f = 1.0).

the velocity causes reduction in heat transfer [26]. Figure 6 also shows that the average Nusselt number increases as the Grashof number increases.

Velocity Distribution

The horizontal velocity distribution along the x-axis (u) in the middle of the cavity above the cylinder at y = 1.25, for different Grashof numbers without and with the presence of fibrous porous material, is depicted in Fig. 7 and Fig. 8,

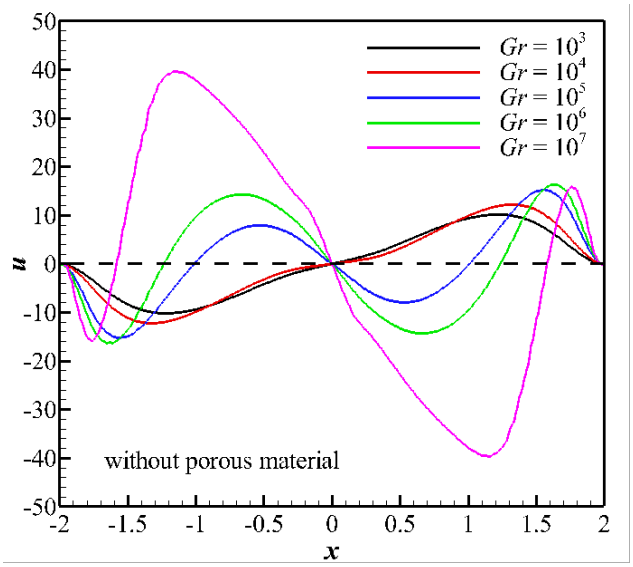

Figure 7. Horizontal velocity distribution along x in the middle of the cavity above the cylinder at y = 1.25, for different Grashof numbers without the presence of porous material.

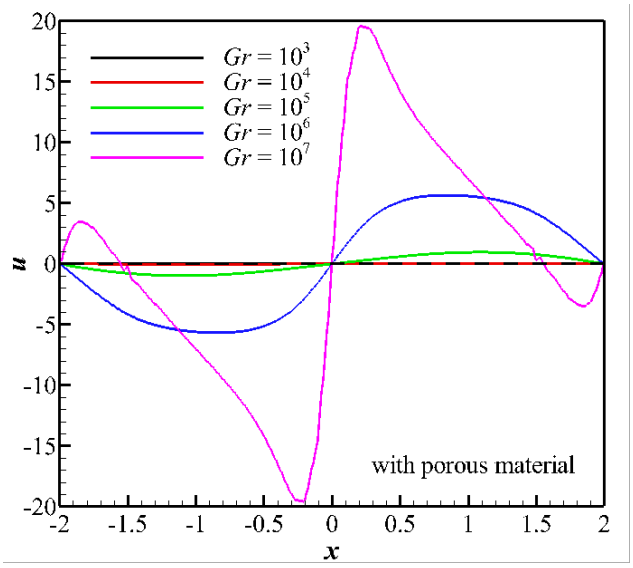

Figure 8. Horizontal velocity distribution along x in the middle of the cavity above the cylinder at y = 1.25, for different Grashof numbers with the presence of porous material.

respectively. For the case of the cavity without porous material, the reverse flow occurs for $G = 10^5$, 10^6, and 10^7 at x = –1, –1.8, and –1.5, respectively. The horizontal velocity increases as Gr increases until it becomes zero at x = 0 (middle of the cavity), and then it begins to decrease (reverse flow) as Gr increases. After that, it returns to increase again and then decreases to be equal to zero at x = 2. While for low Grashof number (10^3 and 10^4), the horizontal velocity distribution is more stable than at Gr > 10^4. If these results are compared with the results of the cavity with a porous material, as can be noticed in Fig. 8, it is seen that the horizontal velocity will be nearly zero for Gr ≤ 10^5. With increasing Gr, the fluid flow in free space is gradually got enhanced, and the velocity boundary layer gradually gets thin. Along with the further increase of Grashof number, the natural convection heat transfer in porous media becomes stronger. The horizontal velocity decreases to its half value in the case of the cavity without fibrous porous media for Gr = 10^6 and 10^7.

The vertical velocity distribution along the x-axis (v) in the middle of the cavity above the cylinder at y = 1.25, for different Grashof numbers without and with the presence of fibrous porous material, is revealed in Fig. 9 and Fig. 10, respectively. For the case of the cavity without fibrous porous material, the maximum vertical velocity occurs at the middle of the cavity middle (x = 0), and this value increases as Gr increases. In contrast, the reverse flow occurs near the sidewalls. Generally, the rates of vertical velocity are higher than the horizontal velocity, especially at higher Grashof numbers. For the case of the cavity with a porous material, the vertical velocity is almost equal to zero for Gr ≤ 10^5. It begins to increase for Gr = 10^6 and 10^7 but with its half value for the case of the cavity without porous material. Indeed,

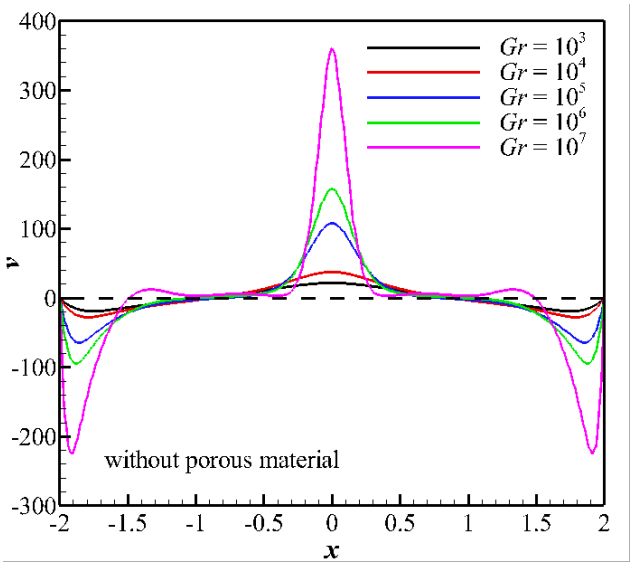

Figure 9. Vertical velocity distribution along x in the middle of the cavity above the cylinder at y = 1.25, for different Grashof numbers without the presence of porous material.

this is clear from the momentum equation of porous media. The terms of Darcy and Forcheimer in Eq. (4) are negative and reduce the (u) and (v) values. In addition, the reverse vertical velocity happens at the sidewalls of the cavity. Generally, the increase of Grashof number means an intensive motivation of free convection and vortex intensity.

Temperature Distribution

Figure 11 shows the temperature distribution along the x-axis with various values of thermal conductivity ratios at y = 1.25, Gr = 5×10^6 and 10^7. It is evidence that the developing temperature values reduce with increasing the thermal conductivity of porous medium because the reduction of wall-cup temperature difference enhances the rate of heat transfer. This behavior reverses at Gr = 10^7 in which the highest maximum temperature is identical for the thermal conductivities k_r = 1, 5, and 7.5, whereas the lowest maximum temperature occurs at k_r = 0.1 and then at 0.5 with a steep temperature gradient near the vertical centerline of the cavity. Generally, the maximum temperature occurs at the mid of the cavity, so the steep temperature gradient occurs for all cases close to the heated wall of the cylinder towards the vertical walls. This behavior is due to the free convection effects, which is weak in the region near the cavity wall because of no appreciable temperature variations in this region. Figure 11 also shows that the thickness of the thermal boundary layer gradually increases with decreasing k_r.

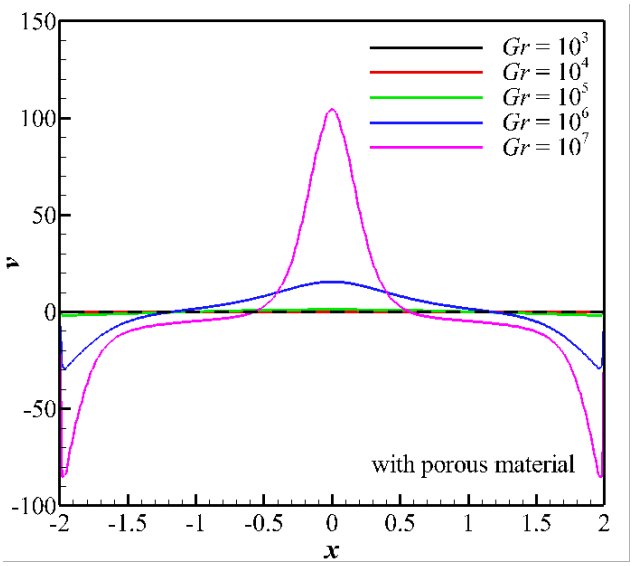

Figure 10. Vertical velocity distribution along x in the middle of the cavity above the cylinder at y = 1.25, for different Grashof numbers with the presence of porous material.

CONCLUSION

The numerical simulation of a steady laminar natural convection heat transfer from a heated circular cylinder to its square enclosure has been conducted. Depending on the results of this study, the following conclusions can be given as follows:

- The strength of the vortex with porous media is stronger than that without porous media for all Rayleigh numbers.
- The centers of identical vortices inside the enclosure with and without porous media are located at the upper and middle parts of the enclosure, respectively, and move upward as Rayleigh number increases.
- At higher values of Rayleigh number, the convection effect in the heat transfer becomes more significant, and the plume begins to appear on the top of the inner cylinder.

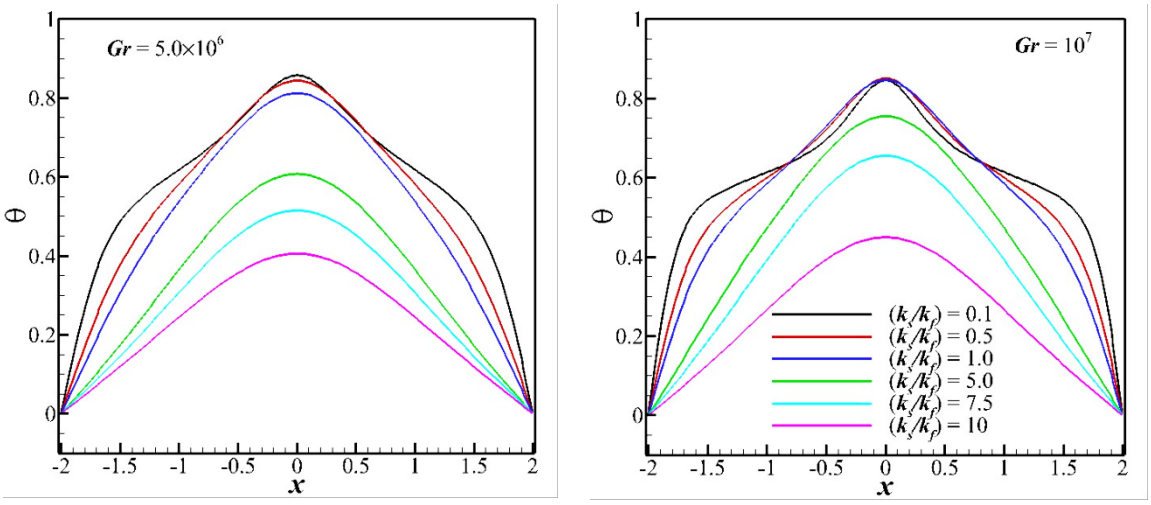

(a) *Gr* = 5 × 10^6 (b) *Gr* = 10^6

Figure 11. Temperature distribution along x in the middle of the cavity above the cylinder at y = 1.25, at the Grashof number of (a) 5×10^6 and (b) 10^7.

- The average values of the horizontal and vertical velocities of the fluid are higher in the case of the enclosure without porous media than that with porous media.
- The developing temperature values reduce with increasing the thermal conductivity of porous medium.
- The maximum temperature occurs at the mid of the enclosure, so the steep temperature gradient occurs for all cases close to the heated wall of the cylinder towards the vertical walls.
- The presence of fibrous porous material with low thermal conductivity relative to the fluid ($k_s = k_f$) and low Darcy number (Da = 10^{-2}) leads to an impermeable medium, which means slow motion of natural convection and lower heat transfer rate than that without porous media.

NOMENCLATURE

C_f	Inertia coefficient = $\frac{1.75}{150\varepsilon^3}$
d	Cylinder diameter
Da	Darcy number,
g	Gravity acceleration (m/s^2)
Gr	Grashof number = $\frac{g\beta d^3(T_h - T_c)}{\vartheta^2}$
h	Average heat transfer coefficient (W/m^2.°C)
h_f	Local heat transfer coefficient (W/m^2.°C)
k_f	Fluid thermal conductivity (W/m.°C)
$k_{f.eff}$	Effective conductivity of fluid.
Nu	Average Nusselt number = hD_h/K
p	Perimeter (m)
P	Pressure field
Pr	Prandtl number = $\mu c_p/K$
Ra	Rayleigh number = Gr.Pr
RR	Hydraulic radius ratio
T	Temperature (°C)
ΔT	Temperature difference (m)
T_h	Hot cylinder temperature
T_c	Cold cavity wall temperature
U	Velocity vector field
u	Horizontal velocity
v	Vertical velocity
L	Square cavity length
x	Horizontal axis
y	Vertical axis

Greek symbols

θ	Dimensionless temperature field $\left(\frac{T - T_c}{T_h - T_c}\right)$
φ	Rotation angle of inner cylinder (rad)
α	Thermal diffusivity (m^2/s)
β	Volume coefficient of expansion (k^{-1})
υ	Kinematical viscosity (m^2/s)
μ	Dynamic viscosity (Pa.s)
ρ	Density (kg/m^3)
κ	Thermal conductivity of air (W/m^2.°C)
ε	Material porosity

AUTHORSHIP CONTRIBUTIONS

Concept: ; Design: ; Materials: ; Data: Analysis: ; Literature search: ; Writing: ; Critical revision:

DATA AVAILABILITY STATEMENT

No new data were created in this study. The published publication includes all graphics collected or developed during the study.

CONFLICT OF INTEREST

The author declared no potential conflicts of interest with respect to the research, authorship, and/or publication of this article.

ETHICS

There are no ethical issues with the publication of this manuscript

REFERENCES

[1] Dalal A, Das MK. Laminar natural convection in an inclined complicated cavity with spatially variable wall temperature. International Journal of Heat and Mass Transfer 2005;48:3833–54. [CrossRef]

[2] Ding H, Shu C, Yeo KS, Lu ZL. Simulation of natural convection in eccentric annuli between a square outer cylinder and a circular inner cylinder using local MQ-DQ method. Numerical Heat Transfer, Part A: Applications 2005;47:291–313. [CrossRef]

[3] Mezrhab A, Jami M, Abid C, Bouzidi MH, Lallemand P. Lattice-Boltzmann modelling of natural convection in an inclined square enclosure with partitions attached to its cold wall. International Journal of Heat and Fluid Flow 2006;27:456–465. [CrossRef]

[4] Varol Y, Oztop HF, Yilmaz T. Two-dimensional natural convection in a porous triangular enclosure with a square body. International communications in heat and mass transfer. 2007;34:238–247. [CrossRef]

[5] Ben-Nakhi A, Chamkha AJ. Conjugate natural convection in a square enclosure with inclined thin fin of arbitrary length", International Journal of Thermal Sciences 2007;46:467–78. [CrossRef]

[6] Oztop HF, Abu-Nada E. Numerical study of natural convection in partially heated rectangular enclosures filled with nanofluids. International Journal of Heat and Fluid Flow 2008;29:1326–36. [CrossRef]

[7] Xu X, Sun G, Yu Z, Hu Y, Fan L, Cen K. Numerical investigation of laminar natural convective heat transfer from a horizontal triangular cylinder to its concentric cylindrical enclosure. International Journal of Heat and Mass Transfer 2009;52:3176–86. [CrossRef]

[8] Hussain SH., Hussein AK. Numerical investigation of natural convection phenomena in a uniformly heated circular cylinder immersed in square enclosure filled with air at different vertical locations. International Communications in Heat and Mass Transfer 2010;37:1115–26. [CrossRef]

[9] Yu ZT., Xu X., Hu YC., Fan LW., Cen KF. Unsteady natural convection heat transfer from a heated horizontal circular cylinder to its air-filled coaxial triangular enclosure. International Journal of Heat and Mass Transfer 2011;54:1563–71. [CrossRef]

[10] Sheikholeslami M, Hashim I, Soleimani S. Numerical investigation of the effect of magnetic field on natural convection in a curved-shape enclosure. Mathematical Problems in Engineering 2013;1-10. [CrossRef]

[11] Balamurugan S, Krishnakanth K. Numerical Study of Convective Heat Transfer for Different Shapes of Hot Sources inside an Enclosure. Research and Reviews: Journal of Engineering and Technology RRJET 2015;4:18–34.

[12] Ravnik J, Škerget L. A numerical study of nanofluid natural convection in a cubic enclosure with a circular and an ellipsoidal cylinder. International Journal of Heat and Mass Transfer 2015;89:596–605. [CrossRef]

[13] Chowdhury R, Khan MAH, Siddiki MNAA. Natural convection in porous triangular enclosure with a circular obstacle in presence of heat generation. American Journal of Applied Mathematics 2015;3:51–58. [CrossRef]

[14] Yuan X, Tavakkoli F, Vafai K. Analysis of natural convection in horizontal concentric annuli of variable inner shape. Numerical Heat Transfer, Part A 2015;68:1155–74. [CrossRef]

[15] Ho YT, Yu TH, Lin KC. Laminar natural convection over a heated cylinder in a cubic – a Lattice Boltzmann study. Proceedings of IASTEM International Conference, Chengdu, China, 17th–18th Jun 2017, 4–8.

[16] Gangawane KM., Manikandan B. Laminar natural convection characteristics in an enclosure with heated hexagonal block for non-Newtonian power law fluids. Chinese Journal of Chemical Engineering 2017;25:555–71. [CrossRef]

[17] Zadkhast M., Toghraie D., Karimipour A. Developing a new correlation to estimate the thermal conductivity of MWCNT-CuO/water hybrid nanofluid via an experimental investigation. J Therm Anal Calorim 2017;129:859–867. [CrossRef]

[18] Abdulkadhim A, Abed AM, Mohsen AM, Al-Farhany K. Effect of partially thermally active wall on natural convection in porous enclosure. Mathematical Modeling of Engineering Problems 2018;5:395-406. [CrossRef]

[19] Geridönmez BP. Numerical simulation of natural convection in a porous cavity filled with free of fluid in presence of magnatic source. Journal of Thermal Engineering 2018;4:1756–69. [CrossRef]

[20] Ataei-Dadavi I, Chakkingal M, Kenjeres S, Kleijn CR, Tummers MJ. Flow and heat transfer measurements in natural convection in coarse-grained porous media. International Journal of Heat and Mass Transfer 2019;130:575–84. [CrossRef]

[21] Zahmatkesh I, Ardekani RA. Effect of magnetic field orientation on nanofluid free convection in a porous cavity: A heat visualization study. Journal of Thermal Engineering 2020;6:170–86. [CrossRef]

[22] Fletcher CAJ. Computational Galerkin methods. New York: Springer-Verlag; 1984. [CrossRef]

[23] Pop I., Kumari M, Nath G. Free convection about cylinders of elliptic cross section embedded in a porous medium. International Journal of Engineering Sciences 1992;30:35–45. [CrossRef]

[24] Yih K. Coupled heat and mass transfer by natural convection adjacent to a permeable horizontal cylinder in a saturated porous medium. International Communications of Heat and Mass Transfer 1999;26:431–440. [CrossRef]

[25] Kumari M, Jayanthi S. Non-darcy non-newtonian free convection flow over a horizontal cylinder in a saturated porous medium. International Communications of Heat and Mass Transfer 2004;31:1219-1226. [CrossRef]

[26] Abbas AH, Messaoud H, Saada D, Abdennacer B. Numerical study of laminar natural convection in porous media: Darcy -Brinkman-Forcheimer model. International Conference on Technologies and Materials for Renewable Energy, Environment and Sustainability, TMREES15, Energy Procedia 2015;74:77–86. [CrossRef]